Photoinduced η Pairing in the Hubbard Model

Tatsuya Kaneko,[1] Tomonori Shirakawa,[2,1,3,4] Sandro Sorella,[2,5,3] and Seiji Yunoki[1,3,4]
[1]*Computational Condensed Matter Physics Laboratory, RIKEN Cluster for Pioneering Research (CPR), Wako, Saitama 351-0198, Japan*
[2]*SISSA–International School for Advanced Studies, Via Bonomea 265, 34136 Trieste, Italy*
[3]*Computational Materials Science Research Team, RIKEN Center for Computational Science (R-CCS), Kobe, Hyogo 650-0047, Japan*
[4]*Computational Quantum Matter Research Team, RIKEN Center for Emergent Matter Science (CEMS), Wako, Saitama 351-0198, Japan*
[5]*Democritos Simulation Center CNR–IOM Instituto Officina dei Materiali, Via Bonomea 265, 34136 Trieste, Italy*

(Received 5 September 2018; published 22 February 2019)

By employing unbiased numerical methods, we show that pulse irradiation can induce unconventional superconductivity even in the Mott insulator of the Hubbard model. The superconductivity found here in the photoexcited state is due to the η-pairing mechanism, characterized by staggered pair-density-wave oscillations in the off-diagonal long-range correlation, and is absent in the ground-state phase diagram; i.e., it is induced neither by a change of the effective interaction of the Hubbard model nor by simple photocarrier doping. Because of the selection rule, we show that the nonlinear optical response is essential to increase the number of η pairs and thus enhance the superconducting correlation in the photoexcited state. Our finding demonstrates that nonequilibrium many-body dynamics is an alternative pathway to access a new exotic quantum state that is absent in the ground-state phase diagram, and also provides an alternative mechanism for enhancing superconductivity.

DOI: 10.1103/PhysRevLett.122.077002

Recent experiments have clearly demonstrated that nonequilibrium dynamics can induce many intriguing phenomena in condensed-matter materials [1–5]. Among them, the most striking is the discovery of photoinduced transient superconducting behaviors in some high-T_c cuprates [6–8] and alkali-doped fullerenes [9,10]. It has also been theoretically shown that superconductivity can be enhanced or induced by pulse irradiation in models for these materials [11–14]. In these studies, the main focus is a photoinduced state with physical properties already present in the corresponding equilibrium phases. In the case of a Mott insulator (MI), photoinduced insulator-to-metal transitions have been reported in time-resolved experiments for several transition-metal and organic-molecular compounds [15–19]. In the MI, the photoinduced metallic state has been recognized as a result of photocarrier doping by creating doublon-holon pairs with no peculiar electronic states emerging [20–22].

In this Letter, we show that pulse irradiation can induce superconductivity even in the celebrated MI of the Hubbard model. The photoinduced superconductivity is due to the η-pairing mechanism, forming on-site singlet pairs that exhibit, unlike conventional s-wave superconductivity, the staggered off-diagonal long-range correlation with a phase of π. Because of the selection rule, the nonlinear optical response is essential to increasing the number of η pairs, and thus enhancing the superconducting correlation. Therefore, our finding is distinct from the previous studies [23–26] and provides an alternative mechanism for enhancing superconductivity via nonequilibrium dynamics.

To demonstrate that superconductivity can be photoinduced in a MI, here we consider the half-filled one-dimensional (1D) Hubbard model at zero temperature. However, our finding does not depend on spatial dimensionality [26]. The model is described by the following Hamiltonian:

$$\hat{\mathcal{H}} = -t_h \sum_{i,\sigma} (\hat{c}^\dagger_{i,\sigma} \hat{c}_{i+1,\sigma} + \mathrm{H.c.}) + U \sum_i \hat{n}_{i,\uparrow} \hat{n}_{i,\downarrow}, \qquad (1)$$

where $\hat{c}_{i,\sigma}$ ($\hat{c}^\dagger_{i,\sigma}$) is the annihilation (creation) operator for an electron at site i with spin $\sigma(=\uparrow,\downarrow)$, and $\hat{n}_{i,\sigma} = \hat{c}^\dagger_{i,\sigma}\hat{c}_{i,\sigma}$. t_h is the hopping integral between the nearest-neighboring sites, while $U(>0)$ is the on-site repulsive interaction. At half-filling, the ground state (GS) of the repulsive 1D Hubbard model is the MI with strong antiferromagnetic correlations.

A time-dependent external field is introduced via the Peierls phase in Eq. (1) by replacing $t_h \hat{c}^\dagger_{i,\sigma}\hat{c}_{i+1,\sigma} \to t_h e^{iA(t)} \hat{c}^\dagger_{i,\sigma}\hat{c}_{i+1,\sigma}$ [36], where $A(t)$ is the vector potential as a function of time t, and the light velocity c, the elementary charge e, the Planck constant $\hbar$, and the lattice constant are set to 1. We consider a pump pulse given as $A(t) = A_0 e^{-(t-t_0)^2/(2\sigma_p^2)} \cos[\omega_p(t-t_0)]$ with the amplitude

 © 2019 American Physical Society

A_0, the frequency ω_p, and the pulse width σ_p centered at time $t_0(>0)$ [37–41]. With finite $A(t)$, the Hamiltonian becomes time dependent, $\hat{\mathcal{H}} \to \hat{\mathcal{H}}(t)$, and the equilibrium GS of $\hat{\mathcal{H}}$ at $t=0$ evolves in time, indicated here by $|\Psi(t)\rangle$. We employ the time-dependent exact diagonalization (ED) method for a finite-size cluster of L (even) sites with periodic boundary conditions (PBC) to solve the time-dependent Schrödinger equation [26]. We set t_h (t_h^{-1}) as a unit of energy (time) and the total number N of electrons to be L at half-filling.

Enhancement of the double occupancy $n_d(t) = (1/L)\sum_i \langle\Psi(t)|\hat{n}_{i,\uparrow}\hat{n}_{i,\downarrow}|\Psi(t)\rangle$ has been already reported in photoexcited states of the MIs [40,42–44]. Here, we find a significant increase of the superconducting pair correlation for the on-site singlet pair $\hat{\Delta}_i = \hat{c}_{i,\uparrow}\hat{c}_{i,\downarrow}$ after the pulse irradiation. Figure 1(a) shows the time evolution of the real-space pair-correlation function defined as $P(j,t) = (1/L)\sum_i \langle\Psi(t)|(\hat{\Delta}^\dagger_{i+j}\hat{\Delta}_i + \mathrm{H.c.})|\Psi(t)\rangle$. Notice that $P(j,t)$ at $j=0$ corresponds to the double occupancy, i.e., $P(j=0,t) = 2n_d(t)$. We thus confirm the enhancement of $n_d(t)$ by the pulse irradiation. Surprisingly, $P(j\neq 0,t)$ is also enhanced significantly by the pulse irradiation and oscillates with the opposite phases between odd and even sites.

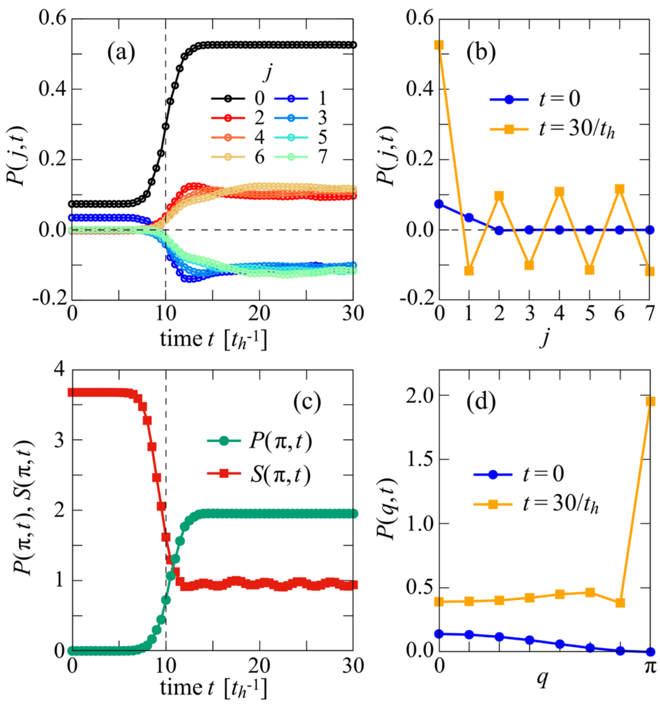

FIG. 1. (a) Time evolution of the on-site pair-correlation function $P(j,t)$. (b) $P(j,t)$ at $t=0$ and $30/t_h$. (c) Time evolution of the pair structure factor $P(q,t)$ and the spin structure factor $S(q,t)$ at $q=\pi$. (d) $P(q,t)$ at $t=0$ and $30/t_h$. The results are calculated by the ED method for $L=14$ at $U=8t_h$ with $A_0=0.4$, $\omega_p=8.2t_h$, $\sigma_p=2/t_h$, and $t_0=10/t_h$.

As shown in Fig. 1(b), the pair correlation after the pulse irradiation extends to longer distances over the cluster, while the pair correlation is essentially absent in the initial MI state before the pulse irradiation. It is also clear that the sign of $P(j,t)$ alternates between neighboring sites, similar to a density wave, and accordingly the pair structure factor $P(q,t) = \sum_j e^{iqR_j}P(j,t)$, where R_j is the location of site j, shows a sharp peak at $q=\pi$ [see Fig. 1(d)]. The time evolution of $P(q,t)$ and the spin structure factor $S(q,t) = \sum_j e^{iqR_j}S(j,t)$, where $S(j,t) = (1/L)\sum_i\langle\Psi(t)|\hat{m}^z_{i+j}\hat{m}^z_i|\Psi(t)\rangle$ and $\hat{m}^z_i = \hat{n}_{i,\uparrow} - \hat{n}_{i,\downarrow}$, is also calculated at $q=\pi$ in Fig. 1(c). The antiferromagnetic correlation $S(q=\pi,t)$ is suppressed by the pulse irradiation, while the pair correlation $P(q=\pi,t)$ is strongly enhanced despite the fact that it is exactly zero before the pulse irradiation. Our matrix product state calculations also find the large enhancement of the pair correlation even for larger clusters that cannot be treated by the ED method [26].

In order to identify the optimal control parameters for the enhancement of $P(q=\pi,t)$, Fig. 2(a) shows the contour plot of $P(\pi,t)$ after the pulse irradiation with different values of A_0 and ω_p. For small A_0, we find that the peak structure of $P(q=\pi,t)$ as a function of ω_p is essentially the same as the GS optical spectrum $\chi_{JJ}(\omega) = (1/L)\langle\psi_0|\hat{J}\delta(\omega-\hat{\mathcal{H}}+E_0)\hat{J}|\psi_0\rangle$, where $|\psi_0\rangle$ is the GS of $\hat{\mathcal{H}}$ with its energy E_0 and $\hat{J} = it_h\sum_{i,\sigma}(\hat{c}^\dagger_{i+1,\sigma}\hat{c}_{i,\sigma} - \hat{c}^\dagger_{i,\sigma}\hat{c}_{i+1,\sigma})$ is the current operator [see Fig. 2(b)]. This agreement is highly nontrivial, and the reason will be clear below. $P(q=\pi,t)$ after the pulse

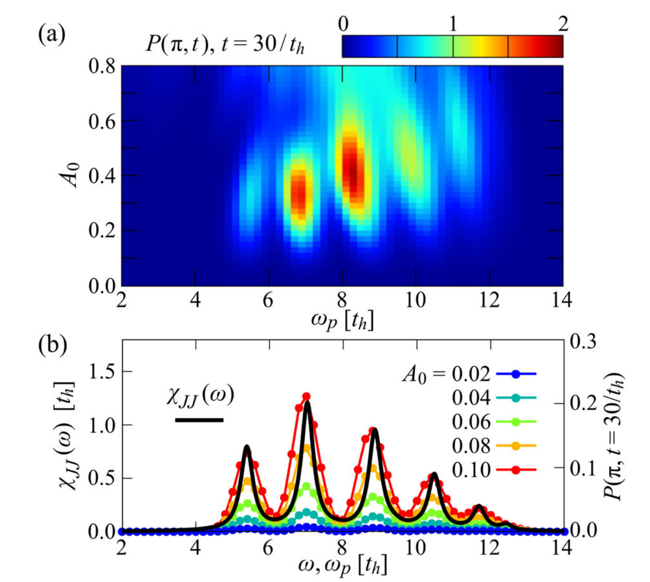

FIG. 2. (a) Contour plot of the pair structure factor $P(q=\pi,t)$ at $t=30/t_h$ with varying ω_p and A_0. (b) The GS optical spectrum $\chi_{JJ}(\omega)$ is compared with $P(q=\pi,t=30/t_h)$ as a function of ω_p for different values of A_0. The results are calculated by the ED method for $L=14$ at $U=8t_h$, with $\sigma_p=2/t_h$ and $t_0=10/t_h$.

irradiation is the largest at $A_0 \sim 0.4$ and $\omega_p \sim 8t_h(= U)$. We should emphasize that the enhancement of $P(q=\pi,t)$ cannot be explained simply by the photodoping of carriers into the MI or due to a dynamical phase transition induced by effectively varying the model parameters, because there is no region in the GS phase diagram of the Hubbard model showing large on-site pairing correlations.

Instead, the behavior of the on-site pairs in the photoinduced state shown in Fig. 1 can be understood in terms of the so-called η-pairing, a concept originally introduced by Yang [45]. In order to define the η-pairing, let us first introduce the following operators: $\hat{\eta}_j^+ = (-1)^j \hat{c}_{j,\downarrow}^\dagger \hat{c}_{j,\uparrow}^\dagger$, $\hat{\eta}_j^- = (-1)^j \hat{c}_{j,\uparrow} \hat{c}_{j,\downarrow}$, and $\hat{\eta}_j^z = \frac{1}{2}(\hat{n}_{j,\uparrow} + \hat{n}_{j,\downarrow} - 1)$. Notice that $\hat{\eta}_j^+$ ($\hat{\eta}_j^-$) is the same as $\hat{\Delta}_j^\dagger$ ($\hat{\Delta}_j$) except for the phase factor. These operators satisfy the $SU(2)$ commutation relations, i.e., $[\hat{\eta}_j^+, \hat{\eta}_j^-] = 2\hat{\eta}_j^z$ and $[\hat{\eta}_j^z, \hat{\eta}_j^\pm] = \pm\hat{\eta}_j^\pm$. Similarly, the total $\hat{\eta}$ operators, $\hat{\eta}^\pm = \sum_j \hat{\eta}_j^\pm$ and $\hat{\eta}_z = \sum_j \hat{\eta}_j^z$, satisfy the $SU(2)$ commutation relations. The essential property of the $\hat{\eta}$ operators here is that they also satisfy $[\hat{\mathcal{H}}, \hat{\eta}^\pm] = \pm U \hat{\eta}^\pm$ with $\hat{\mathcal{H}}$ in Eq. (1).

Yang originally proposed the η-pairing state $|\phi_{N_\eta}\rangle \propto (\hat{\eta}^+)^{N_\eta}|0\rangle$, where $|0\rangle$ is a vacuum with no electrons and N_η is the number of η pairs [45]. Yang's η-pairing state $|\phi_{N_\eta}\rangle$ has two remarkable properties [45]: First, $|\phi_{N_\eta}\rangle$ is an exact eigenstate of the Hubbard model with $2N_\eta$ electrons, satisfying $\hat{\mathcal{H}}|\phi_{N_\eta}\rangle = N_\eta U|\phi_{N_\eta}\rangle$. Second, $\langle\phi_{N_\eta}|\hat{\Delta}_i^\dagger \hat{\Delta}_j|\phi_{N_\eta}\rangle = [N_\eta(L-N_\eta)]/[L(L-1)]e^{i\pi(R_i - R_j)}$ for $i \neq j$, indicating that $|\phi_{N_\eta}\rangle$ exhibits off-diagonal long-range order. Notice that both Yang's η-pairing state $|\phi_{N_\eta}\rangle$ and our photoinduced state $|\Psi(t)\rangle$ show similar sign-alternating characters in the pair-correlation function. However, the photoinduced state $|\Psi(t)\rangle$ excited from the MI state is different from the η-pairing state $|\phi_{N_\eta}\rangle$, in which all electrons participate in forming η pairs, because we find numerically that $|\langle\phi_{N_\eta}|\Psi(t)\rangle|^2 = 0$ at $t = 30/t_h$.

As a candidate of the photoinduced state showing large $P(q=\pi,t)$, we now consider the eigenstate generated from the lowest-weight state (LWS) for $\hat{\eta}$ operators. For this purpose, it is important to notice that $[\hat{\mathcal{H}}, \hat{\eta}^+\hat{\eta}^-] = [\hat{\mathcal{H}}, \hat{\eta}_z] = 0$. Therefore, any eigenstate of $\hat{\mathcal{H}}$ is also the eigenstate $|\eta, \eta_z\rangle$ of $\hat{\eta}^2$ and $\hat{\eta}_z$ with the eigenvalues $\eta(\eta+1)$ and η_z, respectively, where $\hat{\eta}^2 = \frac{1}{2}(\hat{\eta}^+\hat{\eta}^- + \hat{\eta}^-\hat{\eta}^+) + \hat{\eta}_z^2$, $\eta = 0, 1, 2, \ldots, (L/2)$ (at half-filling with the same number of up and down electrons $N_\uparrow = N_\downarrow$), and $\eta_z = -\eta, -\eta+1, \ldots, \eta$. This is precisely the analogue to the total spin operator $\hat{S}$ and its z component $\hat{S}_z$ characterizing any eigenstate of $\hat{\mathcal{H}}$ with $|S, S_z\rangle_{\rm spin}$. The LWS is $|\eta, \eta_z = -\eta\rangle$ and thus satisfies $\hat{\eta}^-|\eta, -\eta\rangle = 0$. Remarkably, Essler *et al.* have shown analytically that all the regular Bethe ansatz eigenstates of the 1D Hubbard model are the LWSs, and the remaining eigenstates can be generated from the LWSs by applying $\hat{\eta}^+$ [46–48].

Following them, we can construct the eigenstate having N_η η pairs from the LWS with $N_\uparrow = N_\downarrow = N_0$ $(\leq L/2)$ as $|\psi_{N_\eta}\rangle = (1/\sqrt{\mathcal{C}_{N_\eta}})(\hat{\eta}^+)^{N_\eta}|\eta = \frac{L}{2} - N_0, \eta_z = -\eta\rangle$ [49]. Yang's η-pairing state $|\phi_{N_\eta}\rangle$ corresponds to $|\psi_{N_\eta}\rangle$ generated from the vacuum state with $N_0 = 0$. At half-filling, $|\psi_{N_\eta}\rangle$ should contain L electrons, and thus we consider $|\psi_{N_\eta}\rangle$ with $N_0 = L/2 - N_\eta$. Therefore, in this case, $|\psi_{N_\eta}\rangle \propto |\eta = N_\eta, \eta_z = 0\rangle$, and hence $\langle\psi_{N_\eta}|\hat{\eta}^+\hat{\eta}^-|\psi_{N_\eta}\rangle = N_\eta(N_\eta+1)$.

As an example, we construct $|\psi_{N_\eta}\rangle$ from the ground state $|\psi_{N_\uparrow,N_\downarrow}^{(\rm GS)}\rangle$ of $\hat{\mathcal{H}}$ with $N_\uparrow = N_\downarrow = N_0$ [51], which is the LWS. Figure 3 shows the on-site pair correlation, $P(j)$ and $P(q)$, for $|\psi_{N_\eta}\rangle$ with different N_η's generated from $|\psi_{N_0,N_0}^{(\rm GS)}\rangle$. The sign-alternating character in $P(j)$ and the enhancement of $P(q=\pi)$ are clearly observed. This is understood because $P(q=\pi) = 2\langle\psi_{N_\eta}|\hat{\eta}^+\hat{\eta}^-|\psi_{N_\eta}\rangle/L = 2N_\eta(N_\eta+1)/L$. With increasing N_η, $|\psi_{N_\eta}\rangle$ crossovers to Yang's η-pairing state $|\phi_{N_\eta=L/2}\rangle$ at $N_\eta = L/2$, for which $P(q=\pi)$ is the largest.

To elucidate the nature of the photoinduced state $|\Psi(t)\rangle$ in terms of the η pairs, we calculate the eigenenergies ε_m and the structure factors $P(q=\pi)$ for all the eigenstates $|\psi_m\rangle$ of $\hat{\mathcal{H}}$ at half-filling. As shown in Fig. 4(a), the structure factor $P(q=\pi)$ for each eigenstate is nicely quantized. This is because each eigenstate $|\psi_m\rangle$ is also the eigenstate of $\hat{\eta}^2$ and $\hat{\eta}_z$, and the quantized values are given as $P(q=\pi) = 2\langle\psi_m|\hat{\eta}^+\hat{\eta}^-|\psi_m\rangle/L = 2\eta(\eta+1)/L$, with $\eta = 0, 1, \ldots, (L/2)$ corresponding to the number of η pairs. These quantized values are exactly the same as $P(q=\pi)$ calculated for $|\psi_{N_\eta}\rangle$ in Fig. 3(b).

In Fig. 4(a), the color of each point indicates the weight $|\langle\psi_m|\Psi(t)\rangle|^2$ of the eigenstate $|\psi_m\rangle$ in the photoinduced state $|\Psi(t)\rangle$ that exhibits the strong enhancement of $P(q=\pi,t)$ after the pulse irradiation [see the inset of

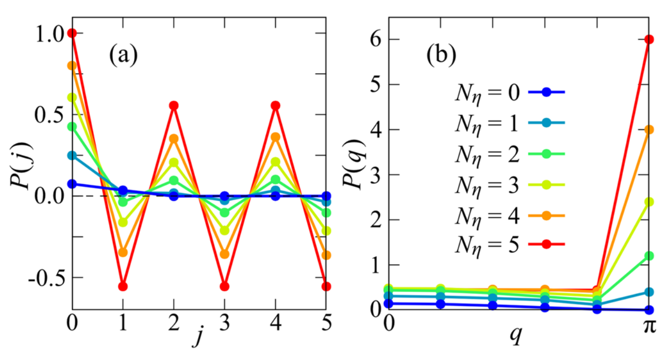

FIG. 3. (a) On-site pair-correlation function $P(j)$ and (b) structure factor $P(q)$ for $|\psi_{N_\eta}\rangle$ at $U = 8t_h$ with the different number of η pairs N_η $(\leq L/2)$. $|\psi_{N_\eta}\rangle$ is generated from the ground state $|\psi_{N_0,N_0}^{(\rm GS)}\rangle$ of $\hat{\mathcal{H}}$ with $N_0 = L/2 - N_\eta$ calculated by the ED for $L = 10$ under PBC.

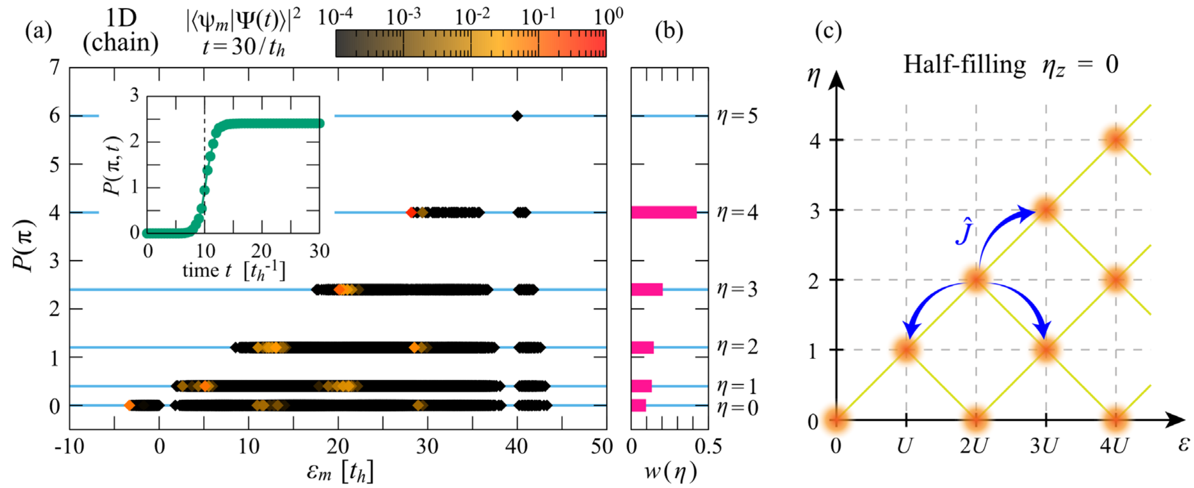

FIG. 4. (a) All eigenenergies ε_m and $P(q=\pi)$ for the eigenstates $|\psi_m\rangle$ of the half-filled Hubbard Hamiltonian $\hat{\mathcal{H}}$ at $U=8t_h$ and $L=10$ under PBC. The color of each point indicates the weight $|\langle\psi_m|\Psi(t)\rangle|^2$ of the eigenstate $|\psi_m\rangle$ in the photoinduced state $|\Psi(t)\rangle$ at $t=30/t_h$ for $A(t)$ with $A_0=0.4$, $\omega_p=7.8t_h$, $\sigma_p=2/t_h$, and $t_0=10/t_h$. The inset shows the time evolution of $P(q=\pi,t)$ for $|\Psi(t)\rangle$. (b) The total weight $w(\eta)$ of $|\langle\psi_m|\Psi(t)\rangle|^2$ over the states $|\psi_m\rangle$ with the same number η of η pairs in (a). Note that $\sum_{\eta=0}^{L/2} w(\eta)=1$. (c) Schematic figure of a "tower of states" $|\psi_m\rangle$ in the photoinduced state $|\Psi(t)\rangle$. The initial state before the pulse irradiation is at $(\varepsilon,\eta)=(0,0)$. The current operator $\hat{J}$ can induce the transition between states with $\Delta\eta=\pm1$ and $\Delta\varepsilon\sim\pm U$, as indicated by arrows, assuming that $\omega_p\sim U$, and thus the pulse irradiation eventually excites a series of states with nonzero η and ε (indicated by orange spheres).

Fig. 4(a)]. We find that the state $|\Psi(t)\rangle$ after the pulse irradiation contains the nonzero weights of the eigenstates $|\psi_m\rangle$ with finite η [also see Fig. 4(b)]. This is exactly the reason for the photoinduced enhancement of $P(q=\pi,t)$. The Hubbard model itself has the eigenstates with $P(q=\pi)\neq 0$, and the photoinduced state $|\Psi(t)\rangle$ captures the weights of those eigenstates.

The process of the enhancement of $P(\pi,t)$ is explained as follows: Before the pulse irradiation, the initial state is the GS of $\hat{\mathcal{H}}$ with $|\eta=0,\eta_z=0\rangle$, i.e., the η singlet state [48], and $P(q=\pi)=0$. The pulse irradiation via $A(t)$ breaks the commutation relation as $[\hat{\mathcal{H}}(t),\hat{\eta}^+]=[\hat{\mathcal{H}},\hat{\eta}^+]+\sum_k F(k,t)\hat{c}^\dagger_{\pi-k,\downarrow}\hat{c}^\dagger_{k,\uparrow}$, with $F(k,t)=4t_h\sin[A(t)]\sin k$, and this transient breaking of the η symmetry stirs states with different values of η. After the pulse irradiation, the Hamiltonian again satisfies the commutation relation because $A(t)=0$, but $|\Psi(t)\rangle$ now contains components of $|\eta\neq 0,\eta_z=0\rangle$, which enhance $P(\pi,t)$.

More precisely, in the small-A_0 limit, the external perturbation is expressed as $A(t)\hat{J}$. We can show that the current operator $\hat{J}$ is a rank-one tensor operator with the zeroth component in terms of the $\hat{\eta}$ operators [26]. Therefore, according to the Wigner-Eckart theorem [52], there exists the selection rule such that $\langle\eta',\eta'_z|\hat{J}|\eta,\eta_z\rangle\neq 0$ only for $\eta'=\eta\pm1$ when $\eta'_z=\eta_z=0$ at half-filling. This implies that in the linear response regime, the photoinduced state $|\Psi(t)\rangle$ can contain the eigenstates $|\psi_m\rangle$ with $\eta=1$ and the eigenenergies $\varepsilon_m\sim U$, assuming that ω_p is tuned around U. This explains the good agreement between the optical spectrum $\chi_{JJ}(\omega)$ and $P(q=\pi,t)$ found in Fig. 2(b). At the second order, the photoinduced state $|\Psi(t)\rangle$ can contain eigenstates $|\psi_m\rangle$ of $\hat{\mathcal{H}}$ with $\eta=2$ and $\varepsilon_m\sim 2U$, as well as $\eta=0$ and $\varepsilon_m\sim 0$ and $2U$. Applying the same argument for higher orders, η-pairing eigenstates with even larger η values acquire in the transient period a finite overlap $|\langle\psi_m|\Psi(t)\rangle|^2$ with the photoinduced state. Considering all orders, eventually, the distribution of eigenstates $|\psi_m\rangle$ in the photoinduced state $|\Psi(t)\rangle$ forms a "tower of states" shown schematically in Fig. 4(c), which is indeed in good qualitative accordance with the numerical results in Fig. 4(a) (for the analysis in the limit of $\sigma_p\to\infty$, see the Supplemental Material [26]). This also explains why the pulse irradiation is effective to induce η pairs, and the nonlinearity is essential to enhance the pair correlation. Note that the nonlinear response is absent in the noninteracting limit, clearly showing the importance of electron correlations.

Exactly the same argument can be applied to the two-dimensional Hubbard model on the square lattice, and indeed we have found the large enhancement of the on-site pairing correlation in the photoinduced state, similar to the 1D case [26]. Although the enhancement of the pair correlation is most effective at half-filling, it remains even away from half-filling [26]. We have also examined the effect of perturbation $\hat{\mathcal{H}}'$ that breaks the η symmetry, i.e., $[\hat{\mathcal{H}}',\hat{\eta}^+\hat{\eta}^-]\neq 0$, and still found the enhancement of the η-pairing correlation specially in the transient period [26].

In conclusion, we have found that density-wave-like staggered superconducting correlations are induced by photoexciting the MI ground state of the half-filled Hubbard model. The superconductivity is due to the η-pairing mechanism where the on-site singlet pairs display off-diagonal long-range correlation with phase π, the fingerprint of the η-pairing state. We have shown that the nonlinear optical response is essential to increase the number of η pairs and hence enhance the superconducting correlation. The η-pairing states were originally introduced purely for the mathematical purpose to solve the Hubbard model analytically, and here we have demonstrated that the pulse irradiation can bring this object into the real world to be observed experimentally.

Finally, we note that a more realistic treatment of materials should include a coupling with other degrees of freedom such as phonons, which introduces slow timescale dynamics in the thermalization process. Therefore, the η-pairing may be realized experimentally in a transient or prethermal regime. The most ideal system to explore the η-pairing experimentally is a cold fermionic atom system, for which the antiferromagnetic order has been recently observed [53].

The authors acknowledge S. Sota, K. Seki, S. Miyakoshi, T. Oka, S. Kitamura, P. Werner, Y. Murakami, and S. Ishihara for fruitful discussion. This work was supported in part by Grants-in-Aid for Scientific Research from MEXT Japan under Grants No. JP17K05523, No. JP18K13509, and No. JP18H01183. T. S. acknowledges the Simons Foundation for financial support (Grant No. 534160). The authors are grateful for providing computational resources of the K computer in RIKEN R-CCS through the HPCI System Research Project (Projects No. hp140130, No. hp150140, No. hp170324, and No. hp180098). The calculations were also performed in part on the RIKEN supercomputer system (HOKUSAI GreatWave) at the Advanced Center for Computing and Communications (ACCC), RIKEN.

[1] Y. Tokura, J. Phys. Soc. Jpn. **75**, 011001 (2006).
[2] S. Iwai and H. Okamoto, J. Phys. Soc. Jpn. **75**, 011007 (2006).
[3] K. Yonemitsu and K. Nasu, Phys. Rep. **465**, 1 (2008).
[4] H. Aoki, N. Tsuji, M. Eckstein, M. Kollar, T. Oka, and P. Werner, Rev. Mod. Phys. **86**, 779 (2014).
[5] C. Giannetti, M. Capone, D. Fausti, M. Fabrizio, F. Parmigiani, and D. Mihailovic, Adv. Phys. **65**, 58 (2016).
[6] D. Fausti, R. I. Tobey, N. Dean, S. Kaiser, A. Dienst, M. C. Hoffmann, S. Pyon, T. Takayama, H. Takagi, and A. Cavalleri, Science **331**, 189 (2011).
[7] W. Hu, S. Kaiser, D. Nicoletti, C. R. Hunt, I. Gierz, M. C. Hoffmann, M. Le Tacon, T. Loew, B. Keimer, and A. Cavalleri, Nat. Mater. **13**, 705 (2014).
[8] S. Kaiser, C. R. Hunt, D. Nicoletti, W. Hu, I. Gierz, H. Y. Liu, M. Le Tacon, T. Loew, D. Haug, B. Keimer, and A. Cavalleri, Phys. Rev. B **89**, 184516 (2014).
[9] M. Mitrano, A. Cantaluppi, D. Nicoletti, S. Kaiser, A. Perucchi, S. Lupi, P. Di Pietro, D. Pontiroli, M. Riccò, S. R. Clark, D. Jaksch, and A. Cavalleri, Nature (London) **530**, 461 (2016).
[10] A. Cantaluppi, M. Buzzi, G. Jotzu, D. Nicoletti, M. Mitrano, D. Pontiroli, M. Riccò, A. Perucchi, P. Di Pietro, and A. Cavalleri, Nat. Phys. **14**, 837 (2018).
[11] M. A. Sentef, A. F. Kemper, A. Georges, and C. Kollath, Phys. Rev. B **93**, 144506 (2016).
[12] D. M. Kennes, E. Y. Wilner, D. R. Reichman, and A. J. Millis, Nat. Phys. **13**, 479 (2017).
[13] K. Ido, T. Ohgoe, and M. Imada, Sci. Adv. **3**, e1700718 (2017).
[14] G. Mazza and A. Georges, Phys. Rev. B **96**, 064515 (2017).
[15] S. Iwai, M. Ono, A. Maeda, H. Matsuzaki, H. Kishida, H. Okamoto, and Y. Tokura, Phys. Rev. Lett. **91**, 057401 (2003).
[16] H. Okamoto, H. Matsuzaki, T. Wakabayashi, Y. Takahashi, and T. Hasegawa, Phys. Rev. Lett. **98**, 037401 (2007).
[17] H. Uemura, H. Matsuzaki, Y. Takahashi, T. Hasegawa, and H. Okamoto, J. Phys. Soc. Jpn. **77**, 113714 (2008).
[18] H. Okamoto, T. Miyagoe, K. Kobayashi, H. Uemura, H. Nishioka, H. Matsuzaki, A. Sawa, and Y. Tokura, Phys. Rev. B **82**, 060513 (2010).
[19] H. Okamoto, T. Miyagoe, K. Kobayashi, H. Uemura, H. Nishioka, H. Matsuzaki, A. Sawa, and Y. Tokura, Phys. Rev. B **83**, 125102 (2011).
[20] T. Oka and H. Aoki, Phys. Rev. B **78**, 241104 (2008).
[21] T. Oka, Phys. Rev. B **86**, 075148 (2012).
[22] M. Eckstein and P. Werner, Phys. Rev. Lett. **110**, 126401 (2013).
[23] A. Rosch, D. Rasch, B. Binz, and M. Vojta, Phys. Rev. Lett. **101**, 265301 (2008).
[24] J.-S. Bernier, P. Barmettler, D. Poletti, and C. Kollath, Phys. Rev. A **87**, 063608 (2013).
[25] S. Kitamura and H. Aoki, Phys. Rev. B **94**, 174503 (2016).
[26] See Supplemental Material at http://link.aps.org/supplemental/10.1103/PhysRevLett.122.077002 for details, which includes Refs. [27–35].
[27] T. J. Park and J. Light, J. Chem. Phys. **85**, 5870 (1986).
[28] N. Mohankumar and S. M. Auerbach, Comput. Phys. Commun. **175**, 473 (2006).
[29] D. Pérez-García, F. Verstraete, M. M. Wolf, and J. I. Cirac, Quantum Inf. Comput. **7**, 401 (2007).
[30] S. R. White, Phys. Rev. Lett. **69**, 2863 (1992).
[31] U. Schollwöck, Ann. Phys. (Amsterdam) **326**, 96 (2011).
[32] M. P. Zaletel, R. S. K. Mong, C. Karrasch, J. E. Moore, and F. Pollmann, Phys. Rev. B **91**, 165112 (2015).
[33] http://itensor.org.
[34] A. G. Rojo, J. O. Sofo, and C. A. Balseiro, Phys. Rev. B **42**, 10241 (1990).
[35] J. Mentink, K. Balzer, and M. Eckstein, Nat. Commun. **6**, 6708 (2015).
[36] R. Peierls, Z. Phys. **80**, 763 (1933).
[37] A. Takahashi, H. Itoh, and M. Aihara, Phys. Rev. B **77**, 205105 (2008).
[38] G. De Filippis, V. Cataudella, E. A. Nowadnick, T. P. Devereaux, A. S. Mishchenko, and N. Nagaosa, Phys. Rev. Lett. **109**, 176402 (2012).

[39] H. Lu, S. Sota, H. Matsueda, J. Bonča, and T. Tohyama, Phys. Rev. Lett. **109**, 197401 (2012).

[40] H. Hashimoto and S. Ishihara, Phys. Rev. B **93**, 165133 (2016).

[41] Y. Wang, M. Claassen, B. Moritz, and T. P. Devereaux, Phys. Rev. B **96**, 235142 (2017).

[42] M. Eckstein and P. Werner, Phys. Rev. B **84**, 035122 (2011).

[43] P. Werner, K. Held, and M. Eckstein, Phys. Rev. B **90**, 235102 (2014).

[44] H. Yanagiya, Y. Tanaka, and K. Yonemitsu, J. Phys. Soc. Jpn. **84**, 094705 (2015).

[45] C. N. Yang, Phys. Rev. Lett. **63**, 2144 (1989).

[46] F. H. L. Essler, V. E. Korepin, and K. Schoutens, Phys. Rev. Lett. **67**, 3848 (1991).

[47] F. H. Essler, V. E. Korepin, and K. Schoutens, Nucl. Phys. **B372**, 559 (1992).

[48] F. H. Essler, H. Frahm, F. Göhmann, A. Klümper, and V. E. Korepin, *The One-Dimensional Hubbard Model* (Cambridge University Press, Cambridge, England, 2005).

[49] $\mathcal{C}_{N_\eta} = N_\eta! \prod_{l=1}^{N_\eta} (L - 2N_0 - l + 1)$ [50].

[50] M. Takahashi, *Thermodynamics of One Dimensional Solvable Models* (Cambridge University Press, Cambridge, England, 1999).

[51] Note that $|\psi_{N_\eta}\rangle$ is the exact eigenstate of $\hat{\mathcal{H}}$ with the eigenenergy $E_{N_0} + N_\eta U$, where E_{N_0} is the eigenenergy of $|\psi^{(\mathrm{GS})}_{N_0,N_0}\rangle$.

[52] J. J. Sakurai, *Modern Quantum Mechanics* (Addison Wesley, Reading, MA, 1994); M. E. Rose, *Elementary Theory of Angular Momentum* (Wiley, New York, 1967).

[53] A. Mazurenko, C. S. Chiu, G. Ji, M. F. Parsons, M. Kanasz-Nagy, R. Schmidt, F. Grusdt, E. Demler, D. Greif, and M. Greiner, Nature (London) **545**, 462 (2017).